Robust Adaptive Contact Force Control of Pantograph–Catenary System: An Accelerated Output Feedback Approach

Yongduan Song, *Fellow, IEEE*, and Luyuan Li

***Abstract*—The pantograph–catenary system plays the crucial role in high-speed electric trains for electrical power collection, where continuity and smoothness of the contact between the pantograph and the catenary is one of the key factors ensuring high-quality power collection essential for safe and reliable train operation. In this article, a nonlinear and highly coupled model for the pantograph–catenary system is established, and an accelerated robust adaptive output feedback control method based on a high-gain observer is proposed to solve the contact force tracking control problem of the pantograph–catenary system using output information only. It is shown that, with the proposed method, the tracking error of the contact force is ensured to be ultimately uniformly bounded with an accelerated preassignable decay rate, resulting in smooth contact force and good-quality current collection. Both theoretical analysis and numerical simulation confirm the effectiveness and benefits of the method.**

***Index Terms*—Accelerated tracking, high-gain observer, pantograph–catenary system, robust adaptive control.**

I. Introduction

THE DRIVING power for high-speed electric trains is obtained through the overhead contact line system, in which the pantograph performs such process continuously during the train operation [1]. Apparently, the pantograph and the catenary comprise a crucial interfacing unit responsible for delivering electrical power to the train [2]. The pantograph is a pneumatic or spring-loaded scaling mechanism connected to the roof by an insulator, and the contact wire is supported by equally spaced vertical droppers suspended from a catenary wire, as shown in Fig. 1. Here, the pantograph and the catenary form a dynamic system with coupling interactions.

Manuscript received December 6, 2019; revised March 11, 2020 and May 22, 2020; accepted June 4, 2020. Date of publication July 15, 2020; date of current version April 27, 2021. This work was supported in part by the National Natural Science Foundation of China under Grant 61860206008, Grant 61773081, Grant 61933012, and Grant 61833013. *(Corresponding author: Yongduan Song.)*

Yongduan Song is with the Chongqing Key Laboratory of Intelligent Unmanned Systems, Chongqing University, Chongqing 400044, China (e-mail: ydsong@cqu.edu.cn).

Luyuan Li is with the Institute of Advanced Control System, School of Electronic and Information Engineering, Beijing Jiaotong University, Beijing 100044, China (e-mail: 17120241@bjtu.edu.cn).

Color versions of one or more of the figures in this article are available online at https://ieeexplore.ieee.org.

Digital Object Identifier 10.1109/TIE.2020.3003547

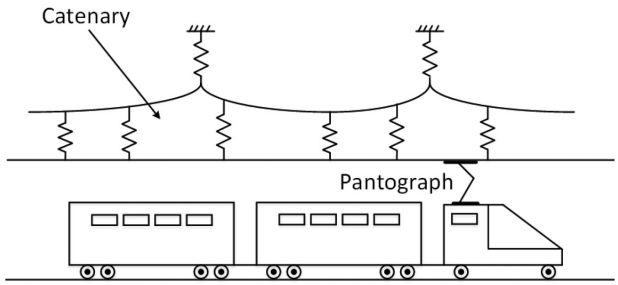

Fig. 1. Pantograph–catenary systems for power collection in high-speed trains.

The decisive criterion for assessing the quality of current feeding of high-speed trains is the same as that for assessing the quality of contact between the pantograph and the catenary. Therefore, this article aims at improving the smoothness and continuity of the contact force that plays an important role in enhancing the quality of electric power collection. The contact force is composed of the static force and the dynamic force, which depends on the running speed and vibration behavior caused by external disturbances. As the speed of the train increases, the vibration of the train body becomes increasingly noticeable [3], which negatively impacts the contact force between the pantograph and the overhead wire of the high-speed train. If not controlling properly, it may lead to a zero contact force, resulting in loss of contact, arcing, and wearing (see[4] and [5]).

The study of controlling the pantograph–catenary system has gained increasing attention from control community during past few years. Most of the existing methods for stabilizing the contact force and improving the quality of current collection in high-speed trains can be broadly classified into two categories: passive and active. The typical passive methods (for example, see [6]) suffer from the shortcomings of excessive contact force (thus extreme wire wearing) or are too expensive to implement in the case of modification of existing railway systems. Therefore, there seems to be a general agreement that active control methods are the mainstream trend of the pantograph–catenary system with great potential in existing railway systems (for example, see [7]–[10]), and fruitful results have been reported in the literature. A robust control of contact force of the pantograph–catenary system has been proposed in [7]. In addition, Song *et al.* [11]

proposed a sliding-mode control with proportional–derivative sliding surface for pantograph–catenary contact force under strong stochastic wind field. In [12], a new continuum-based pantograph–catenary model is proposed and used to develop an effective method to control the contact force and improve the contact quality. It is worth noting that most control methods are based on an oversimplified model of the pantograph–catenary system (for example, see [8]). This may result in lots of limits and problems in practice due to the fact that simple models do not provide sufficient information on system behavior. Another challenge for control design is that some state variables are not directly measurable in contrast to the "fully measurable" assumptions in many articles (for example, see [9], [13], and [14]). It is, therefore, highly desirable to design a control algorithm that is largely model independent and requires little system dynamic information.

In this article, a less model-dependent approach is proposed to regulate the contact force. Compared with most of the existing methods, it avoids linearizing the system and utilizes output feedback only. The main contributions of this article can be summarized as follows.

1) A nonlinear two-degree-of-freedom coupled model of the pantograph–catenary system is developed and utilized for control design, in which no linearization or approximation is needed in deriving the control algorithm.
2) Both modeling uncertainties and external disturbances are taken into account in control design, and the proposed control is able to ensure continuous and smooth contact between the pantograph and the overhead contacting wire, leading to high-quality current collection, as confirmed by formative theoretical analysis and numerical simulations.
3) The technique of a high-gain observer is utilized in control development, which allows the control to be implementable with only output information of the system.
4) By integrating the rate function into the neural adaptive control, the proposed control scheme ensures the contact force tracking error to converge with an accelerated and prespecifiable decay rate.

The rest of this article is organized as follows. Section II presents the modeling of the catenary–pantograph system and the problem formulation. Section III gives some useful preliminaries for the control scheme. In Section IV, the accelerated robust adaptive control scheme based on a high-gain observer is developed with detailed stability analysis. Section V verifies via simulation the effectiveness of the proposed control scheme. Finally, Section VI concludes this article.

II. Modeling and Problem Formulation

A. Modeling of the Pantograph–Catenary System

The pantograph–catenary system is a complex multifactor coupling system. Most studies on control of the pantograph–catenary system are based on simplified mathematical models [15]. Fig. 2(a) represents the typical structure model

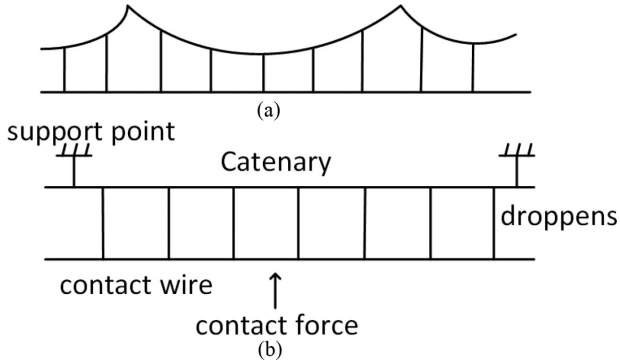

Fig. 2. Model of catenary.

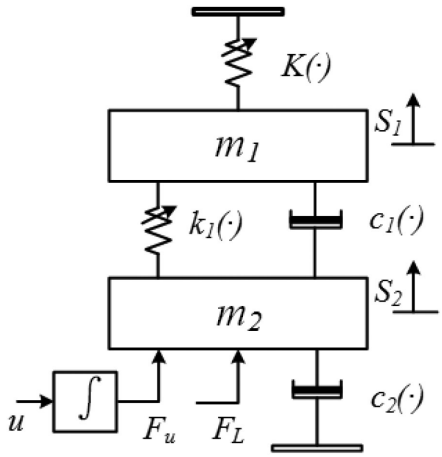

Fig. 3. Two-degree-of-freedom coupled model of the pantograph–catenary system.

of the suspension catenary. Fig. 2(b) shows the simplified model of catenary head, with the related parameters being expressed as $K(\cdot) = K_0 + \Delta K(\cdot)$, where $K_0 = (K_{\max} + K_{\min})/2$, $\Delta K(\cdot) = K_0 \alpha \cos(2\pi V t/L)$, and $\alpha = (K_{\max} - K_{\min})/(K_{\max} + K_{\min})$. Here, $K_{\max}$ and $K_{\min}$ represent the maximum and minimum values of the stiffness change of the catenary within a span, respectively, L is the length of the mesh span of catenary, and V is the speed of the train.

The most common model of pantograph is the centralized quality model, which we used in this article. According to the number of concentrated masses, it is divided into different types. In order to better reflect the kinematics of the pantograph and avoid overly complex mathematical calculations at the same time, here, we choose a binary model (two concentrated masses) to reflect the dynamic characteristics of the pantograph/catenary system. Combined with the catenary model, as conceptually shown in Fig. 3, the two degree-of-freedom model dynamic characteristics can be described by the following equations:

$$\begin{cases} m_1\ddot{s}_1 = \Gamma_1\left(K\left(\cdot\right), c_1\left(\cdot\right), k_1\left(\cdot\right), s_1, \dot{s}_1, s_2, \dot{s}_2\right) + d_1(t) \\ m_2\ddot{s}_2 = \Gamma_2\left(F_u, k_1\left(\cdot\right), c_1\left(\cdot\right), c_2\left(\cdot\right), s_1, \dot{s}_1, s_2, \dot{s}_2\right) \\ \qquad\quad + d_2(t) + F_L \\ f(t) \ = \Gamma_3\left(K\left(\cdot\right), s_1\right) \end{cases} \tag{1}$$

where m_1 and m_2 are the concentrated mass of the pan-head and frame, respectively, s_1 and s_2 are the displacement and velocity of the bow and frame of the pantograph, respectively, $d_1(t)$ and $d_2(t)$ are unknown external disturbances, F_u is the actual control force acting on the lower frame, F_L is the static lift, $f(t)$ is the contact force between the pantograph and the catenary, $k_1(\cdot)$ is the equivalent coefficient of the spring, and $c_1(\cdot)$ and $c_2(\cdot)$ represent the equivalent value of damping coefficient .

Remark 1: In most of the existing methods, the nonlinear terms $\Gamma_1(\cdot)$, $\Gamma_2(\cdot)$, and $\Gamma_3(\cdot)$ in (1) are normally simplified as a linear form (for example, see [9], [13], and[15]). Here, in this work, we consider a nonlinear model as in (1) to better reflect the dynamic behavior of the pantograph–catenary system.

B. Problem Formulation

The contact force tracking control problem investigated in this article can be formulated as follows. For the pantograph–catenary system described by the nonlinear model (1), design a control scheme using output information only to achieve the control objective that the contact force $f(t)$ tracks the desired force $f_d(t)$ closely, where $f_d(t)$ and its derivatives up to the fourth order are bounded for all $t > 0$.

To facilitate the control design and stability analysis, we define $x_1 = f(t) - f_d(t)$, which represents the force tracking error. For notation simplicity, sometimes, $K(\cdot)$, $d_1(t)$, and $d_2(t)$ will be written as K, d_1, and d_2, respectively, if no confusion is likely to occur.

With the definition of x_1, we can express (1) into the following Brunovsky form:

$$\begin{cases} \dot{x}_1(t) = x_2(t) \\ \dot{x}_2(t) = x_3(t) \\ \dot{x}_3(t) = x_4(t) \\ \dot{x}_4(t) = G(\cdot)u + D(\cdot) \\ e_m \quad = x_1 \end{cases} \tag{2}$$

where e_m represents the output (force tracking error of the system)

$$G(\cdot) = \frac{1}{m_1 m_2}\left(\frac{\partial \Gamma_3}{\partial s_1}\right)\left(\frac{\partial \Gamma_1}{\partial \dot{s}_2}\right)\left(\frac{\partial \Gamma_2}{\partial F_u}\right) \tag{3}$$

$$u = \dot{F}_u \tag{4}$$

$$D(\cdot) = \Re(\cdot) - f_d(t)^{(4)} \tag{5}$$

$$\begin{aligned} \Re(\cdot) &= \Re_0(\cdot) \\ &\quad + \frac{\partial \Re_2}{m_2 \partial \dot{s}_2}\Gamma_2(F_u, c_1(\cdot), k_1(\cdot), c_2(\cdot), s_1, \dot{s}_1, s_2, \dot{s}_2) \end{aligned} \tag{6}$$

$$\begin{aligned} \Re_0(\cdot) &= \frac{\partial \Re_2}{\partial s_1}\dot{s}_1 + \frac{\partial \Re_2}{\partial s_2}\dot{s}_2 + \frac{\partial \Re_2}{\partial K}\dot{K} + \frac{\partial \Re_2}{\partial \dot{K}}\ddot{K} + \frac{\partial \Re_2}{\partial \ddot{K}}K^{(3)} \\ &\quad + \frac{\partial \Re_2}{\partial K^{(3)}}K^{(4)} + \frac{\partial \Re_2}{\partial c_1(\cdot)}\dot{c}_1(\cdot) + \frac{\partial \Re_2}{\partial \dot{c}_1(\cdot)}\ddot{c}_1(\cdot) \\ &\quad + \frac{\partial \Re_2}{\partial k_1(\cdot)}\dot{k}_1(\cdot) + \frac{\partial \Re_2}{\partial \dot{k}_1(\cdot)}\ddot{k}_1(\cdot) + \frac{\partial \Re_2}{\partial c_2(\cdot)}\dot{c}_2(\cdot) \\ &\quad + \frac{\partial \Re_2}{\partial d_1}\dot{d}_1 + \frac{\partial \Re_2}{\partial \dot{d}_1}\ddot{d}_1 + \frac{\partial \Re_2}{m_1 \partial \dot{s}_1}d_1 + \frac{\partial \Re_2}{m_2 \partial \dot{s}_2}d_2 \\ &\quad + \frac{\partial \Re_2}{\partial d_2}\dot{d}_2 + \frac{\partial \Re_2}{m_1 \partial \dot{s}_1}\Gamma_1(K, c_1(\cdot), k_1(\cdot), s_1, \dot{s}_1, s_2, \dot{s}_2) \end{aligned} \tag{7}$$

$$\begin{aligned} \Re_2(\cdot) &= \frac{\partial \Re_1}{\partial s_1}\dot{s}_1 + \frac{\partial \Re_1}{\partial s_2}\dot{s}_2 + \frac{\partial \Re_1}{\partial K}\dot{K} + \frac{\partial \Re_1}{\partial \dot{K}}\ddot{K} \\ &\quad + \frac{\partial \Re_1}{\partial c_1(\cdot)}\dot{c}_1(\cdot) + \frac{\partial \Re_1}{\partial k_1(\cdot)}\dot{k}_1(\cdot) + \frac{\partial \Re_1}{\partial \ddot{K}}K^{(3)} \\ &\quad + \frac{\partial \Re_1}{\partial d_1}\dot{d}_1 + \frac{\partial \Re_1}{m_1 \partial \dot{s}_1}d_1 + \frac{\partial \Re_1}{m_2 \partial \dot{s}_2}d_2 \\ &\quad + \frac{\partial \Re_1}{m_1 \partial \dot{s}_1}\Gamma_1(K, c_1(\cdot), k_1(\cdot), s_1, \dot{s}_1, s_2, \dot{s}_2) \\ &\quad + \frac{\partial \Re_1}{m_2 \partial \dot{s}_2}\Gamma_2(F_u, c_1(\cdot), k_1(\cdot), c_2(\cdot), s_1, \dot{s}_1, s_2, \dot{s}_2) \end{aligned} \tag{8}$$

$$\begin{aligned} \Re_1(\cdot) &= \frac{\partial \Re_3}{\partial s_1}\dot{s}_1 + \frac{\partial \Re_3}{\partial K}\dot{K} + \frac{\partial \Re_3}{\partial \dot{K}}\ddot{K} + \frac{\partial \Re_3}{m_1 \partial \dot{s}_1}d_1 \\ &\quad + \frac{\partial \Re_3}{m_1 \partial \dot{s}_1}\Gamma_1(K, c_1(\cdot), k_1(\cdot), s_1, \dot{s}_1, s_2, \dot{s}_2) \end{aligned} \tag{9}$$

$$\Re_3(\cdot) = \frac{\partial \Gamma_3(K, s_1)}{\partial K}\dot{K} + \frac{\partial \Gamma_3(K, s_1)}{\partial s_1}\dot{s}_1. \tag{10}$$

Remark 2: Note that u is the time derivative of F_u; thus, once u is specified, F_u can be obtained by integrating u.

Remark 3: It turns out that $G(\cdot)$ and $D(\cdot)$, as defined in (2), are all quite complex, unknown, and time varying and, thus, cannot be directly used for control design. In this work, we develop a control scheme that does not need the specific information on system model and parameters. Taking into account the overall longitudinal train dynamics, together with the fact that the equivalent catenary stiffness is a smooth function of the train position, it can be deduced that $K(\cdot)$ and its derivatives up to the second order are bounded.

Remark 4: The control objective is achieved if we regulate e_m so that $e_m = x_1 \to 0$ or $|e_m| = |x_1| < \varepsilon_0$ as $t > T_f$.

III. Some Useful Preliminaries

A. Setting and Conditions

Before presenting the control scheme, the following assumptions are required.

Assumption 1: The known desired trajectory f_d and its derivatives up to $(n+1)$th order are all smooth and bounded functions.

Assumption 2: Only the system output is available for control design.

Lemma 1 (see[16] and [17]): For the Gaussian radial basis functions, which have the form $s_i(z) = \exp[-\frac{\|z-\kappa_i\|^2}{\eta_i}] = \exp[-\frac{(z-\kappa_i)^T(z-\kappa_i)}{\eta_i}]$, $i = 1, 2, ..., L_P$, where κ_i is the center of the receptive field, L_p is the weight number and η_i is the width of

the Gaussian function. If $\hat{z} = z - \theta\bar{\psi}$, with $\theta > 0$ being a constant and $\bar{\psi}$ being a bounded vector, then $S(\hat{z}) = S(z) - \theta S_z$, where S_z is a bounded function vector.

B. Rate Function

Definition 1: A real function $k_s(t)$ is a rate function if the following conditions are satisfied [18].

1) $k_s(t)$ is a strictly increasing and positive function of time in $[0, \infty)$ and $k_s(0) = 1$, such that ${k_s}^{-1}(t)$ is strictly decreasing and positive function satisfying $\lim_{t\to\infty} {k_s}^{-1}(t) = 0$.

2) $k_s(t)$ is C^∞ for all $t \in [0, \infty)$.

3) ${k_s}^{-1}(t)$ and its derivatives up to nth$(n \to \infty)$ order is well defined and satisfy $\lim_{t\to\infty} ({k_s}^{-1}(t))^{(i)} = 0 (i = 0, 1, \ldots, \infty)$.

The rate function is introduced and utilized to construct the function β as in (14) to facilitate the development of accelerated tracking control in the following.

C. High-Gain Observer

In actual situations, although the value of the contact force between the pantograph and the catenary can be measured by sensors, other higher order variables such as the change rate of contact force are difficult to measure. Therefore, the internal state variables of system (2) are not available for feedback control; we need to use the high-gain observer for designing the controller. The following result for the high-gain observer is used for later control development.

Lemma 2 (see[19] and [20]): Assume that the output $y(t)$ of a system and its derivatives up to $(n-1)$th order are bounded, i.e., $y^{(k)} \le Y_k$, with $Y_k (k = 0, 1, \ldots, n-1)$ being constants. Consider the following linear system:

$$\begin{cases} \delta\dot{\varsigma}_i = \varsigma_{i+1}, \quad i = 1, 2, \ldots, n-1 \\ \delta\dot{\varsigma}_n = -\mu_1\varsigma_n - \mu_2\varsigma_{n-1} - \cdots - \mu_{n-1}\varsigma_2 - \varsigma_1 + y(t) \end{cases} \tag{11}$$

with $\delta > 0$ being any small constant, where $\varsigma_i, i = 1, 2, \ldots, n$, are the state variables of the observer. Choosing the parameters $\mu_1, \mu_2, \ldots, \mu_{n-1}$ such that the polynomial $s^n + \alpha_1 s^{n-1} + \cdots + \alpha_{n-1}s + 1$ is Hurwitz.

Then, we have the following properties.

1)
$$\frac{\varsigma_{k+1}}{\delta^k} - y^{(k)} = -\delta\varpi^{(k+1)}, \quad k = 0, 1, \ldots, n-1 \tag{12}$$
where $\varpi = \varsigma_n + \alpha_1\varsigma_{n-1} + \cdots + \alpha_{n-1}\varsigma_1$, with $\varpi^{(k+1)}$ denoting the kth derivative of ϖ.

2) There exist positive constants t_0 and b_k that only depend on $\le Y_K, k = 0, 1, \ldots, n-1, \delta$ and μ_i, such that we have $|\varpi^{(k)}| \le b_k$ for all $t \ge t_0$.

Remark 5: From 1) and 2), it holds that $\frac{\varsigma_{k+1}}{\delta^k}$ converges to $y^{(k)}$ with bounded error if y and its derivatives first and up to kth order are bounded. Thus, $\frac{\varsigma_{k+1}}{\delta^k} (k = 0, 1, \ldots, n-1)$ can provide the estimations of the unmeasured derivatives of the output up to the $(n-1)$th order and $|y^{(k)} - \varsigma_{k+1}/\delta^k| \le \delta b_k$, $k = 0, 1, \ldots, n-1$, is established.

IV. Control Design and Stability Analysis

For the nonlinear dynamic system (2), it is nontrivial to build a controller without using $G(\cdot)$ and $D(\cdot)$ directly. It is even more challenging if the output is the only feedback information to use. Here, we use the high-gain observer to estimate the unknown system states.

As noted in [16], the internal dynamics of system (2) is bounded-input bounded-output stable. Furthermore, although $G(\cdot)$ is known precisely, it is straightforward to show that

$$0 < \underline{\lambda}_G \le G(\cdot) \le \bar{\lambda}_G \tag{13}$$

where $\underline{\lambda}_G$ and $\bar{\lambda}_G$ are some unknown constants.

A. Error Dynamics

To proceed, we construct the following time-varying scaling function with the previously defined rate function k_s[18]:

$$\beta(k_s) = \frac{1}{(1 - b_f){k_s}^{-1} + b_f} \tag{14}$$

where b_f is chosen to obey that $0 < b_f << 1$ by the designer, and k_s is given as in Definition 1. It can be easily shown that $\beta(k_s)$ is a monotonically increasing and bounded function of time, where we define the upper bound as $\bar{\beta}$, and its derivatives for any order are smooth and bounded.

Then, we conduct the following transformation on e_m:

$$\xi_1 = \beta e_m \tag{15}$$

and we further define

$$\xi_i = \frac{d}{dt}\xi_{i-1}, \quad i = 2, 3, 4. \tag{16}$$

For subsequent theoretical derivation, instead of defining the filtered error $s = q_1 e_m + q_2 {e_m}^{(1)} + q_3 {e_m}^{(2)} + {e_m}^{(3)}$ [16], we introduce the transformed E as follows:

$$E = q_1\xi_1 + q_2\xi_2 + q_3\xi_3 + \xi_4 \tag{17}$$

where q_i, $i = 1, 2, 3$, are specific constants greater than zero and guarantee that the polynomial $w^3 + q_1 w^2 + q_2 w + q_3$ is Hurwitz. In later stability analysis, we will need to deal with β^2 as in (41); thus, we define $\alpha_1(t) = \beta^2$; using the condition on β, it can be shown that there exist $\underline{\lambda}_1$ and $\bar{\lambda}_1$, such that

$$0 < \underline{\lambda}_1 \le \alpha_1(t) \le \bar{\lambda}_1 < \infty. \tag{18}$$

From (17), we have

$$\begin{aligned} \dot{E} &= \sum_{j=1}^{3} q_i\xi_{j+1} + \sum_{j=0}^{4} C_4^j \beta^{(j)} {e_m}^{(4-j)} \\ &= \beta\dot{x}_4 + \psi \end{aligned} \tag{19}$$

where $\psi = \sum_{j=1}^{3} q_i\xi_{j+1} + \sum_{j=1}^{4} C_4^j \beta^{(j)} {e_m}^{(4-j)}$ is a computable function with $C_4^j = \frac{4!}{j!(4-j)!}$.

Substituting (2) into (19), we then obtain

$$\dot{E} = \beta(Gu + \vartheta) \tag{20}$$

where

$$\begin{aligned}\vartheta &= D(\cdot) + \beta^{-1}\psi \le |D(\cdot)| + \left|\beta^{-1}\psi\right| \\ &\le |D(\cdot)| + \left|\beta^{-1}\right| \sum_{j=1}^{3} q_j \left|\xi_{j+1}\right| \\ &\quad + \left|\beta^{-1}\right| \sum_{j=1}^{4} C_4^j \left|\beta^{(j)}\right| \left|{e_m}^{(4-j)}\right| = \varphi(\cdot)\end{aligned} \tag{21}$$

It is interesting to note that the virtual parametric decomposition of the lumped uncertain ϑ can be dealt with by a neural network (NN)-based method [21]. The NN has been proven capable of approximating unknown nonlinear functions in compact set with sufficient accuracy, and this feature has been used to handle nonlinearities in a variety of nonlinear systems successfully [22], [23]. Hence, we use the NN to reconstruct the upper bound of ϑ as follows:

$$\begin{aligned}\varphi(\cdot) &= W^{*T} S(Z) + \eta(Z) \\ &\le \left\|W^{*T}\right\| \|S(Z)\| + \eta_N(Z) \\ &\le a_0 \Phi_0(Z)\end{aligned} \tag{22}$$

where $W^{*T} \in R^L$ is the optimal weight vector of the radial basis function NN, $\eta(Z)$ is the NN approximation error, and $|\eta(Z)| < \eta_N(Z) < \infty$, which $\eta_N(Z)$ is some unknown constant. Note that in a compact set, if the weight number L_p is large enough, $\eta_N(Z)$ can be arbitrarily small. $S(Z)$ is the basic function, with $Z = X = [x_1, x_2, x_3, x_4]$ being the NN input. $a_0 = \max\{\|W^{*T}\|, \eta_N\}$ is an unknown but bounded constant, and $\Phi_0(Z) = \|S(Z)\| + 1$ related to the input of the NN.

Remark 6: It is interesting to note that there exist direct correlations between the filtered state variable of the system $s_1, \dot{s}_1, s_2, \dot{s}_2$ and the original state variable x_1, x_2, x_3, x_4 through (2)–(10); therefore, we use $X = [x_1, x_2, x_3, x_4]$ instead of $[s_1, \dot{s}_1, s_2, \dot{s}_2]$ as part of the input signals to the NN, and, as shown later on, since X is not completely available, an observer will be constructed to provide an estimation of X (i.e., $\hat{X}$). The feasibility and practicality of such treatment will be analyzed via Lemma 1.

B. Controller Design

To proceed, we design a high-gain observer with the following structure:

$$\begin{cases} \delta\dot{\pi}_1 = \pi_2 \\ \delta\dot{\pi}_2 = \pi_3 \\ \delta\dot{\pi}_3 = \pi_4 \\ \delta\dot{\pi}_4 = -\mu_1\pi_4 - \mu_2\pi_3 - \mu_3\pi_2 - \pi_1 + e_m \end{cases} \tag{23}$$

where $\pi_i, i = 1, 2, 3, 4$, is the state variable of the high-gain observer. According to Lemma 2, the estimated value corresponding to the state vector of the system can be expressed as

$$\hat{x}_i = \frac{1}{\delta^{i-1}}\pi_i, \quad i = 1, 2, 3, 4. \tag{24}$$

As described in Remark 5, we can know the state estimation error of the high-gain observer is bounded, such that the following inequality is obtained:

$$|x_i - \hat{x}_i| = \delta\left|\varpi^{(i)}\right| \le \delta b_i, \quad i = 1, 2, 3, 4. \tag{25}$$

Next, before designing the controller, it is necessary to use the state estimation value $\hat{x}_i$ obtained by the high-gain observer instead of the real state variable x_i in algorithm development. To this end, let us redefine e_m, ξ_i, and E as follows:

$$\hat{e}_m = \hat{x}_1 \tag{26}$$

$$\hat{\xi}_i = \sum_{j=0}^{i-1} C_{i-1}^j \beta^{(j)} \hat{e}_m^{(i-1-j)}, \quad i = 1, 2, 3, 4 \tag{27}$$

$$\hat{E} = q_1\hat{\xi}_1 + q_2\hat{\xi}_2 + q_3\hat{\xi}_3 + \hat{\xi}_4. \tag{28}$$

From (25), we can get $\hat{Z} = Z - \theta\tilde{\varpi}$, with $\hat{Z} = \hat{X} = [\hat{x}_1, \hat{x}_2, \hat{x}_3, \hat{x}_4]$, $\tilde{\varpi} = [\tilde{\varpi}, \ddot{\varpi}, \varpi^{(3)}, \varpi^{(4)}]$, and $\theta = \delta > 0$. According to Lemma 1, it can be shown that there is a bounded function vector S_z such that $S(\hat{Z}) = S(Z) - \theta S_z$ holds, thereby

$$\begin{aligned}\|S(Z)\| &= \left\|S\left(\hat{Z}\right) + \theta S_z\right\| \\ &\le \left\|S\left(\hat{Z}\right)\right\| + \theta\|S_z\| \\ &\le \left\|S\left(\hat{Z}\right)\right\| + \theta s_z\end{aligned} \tag{29}$$

where $s_z > 0$ is the upper bound on $\|S_z\|$. Then, we have

$$\begin{aligned}\varphi(\cdot) &= W^{*T} S(Z) + \eta(Z) \\ &\le \|W^{*T}\|\left(\left\|S\left(\hat{Z}\right)\right\| + \theta s_z\right) + \eta_N(Z) \\ &\le a\Phi\left(\hat{Z}\right)\end{aligned} \tag{30}$$

with $\Phi(\hat{Z}) = \|S(\hat{Z})\| + 2$ and $a = \max\{\|W^{*T}\|, \|W^{*T}\| \theta s_z + \eta_N\}$.

In the subsequent stability analysis, we need the following result.

Proposition: With the proposed high-gain observer (23), $\theta_E = E - \hat{E}$ is bounded.

Proof: According to the previously defined E and $\hat{E}$, it holds that

$$\begin{aligned}\theta_E &= q_1\beta(x_1 - \hat{x}_1) + q_2\left[\dot{\beta}(x_1 - \hat{x}_1) + \beta(x_2 - \hat{x}_2)\right] \\ &\quad + \cdots + q_{i-1}\sum_{j=0}^{i-2} C_{i-2}^j \beta^{(j)}(x_{j+1} - \hat{x}_{j+1}) \\ &\quad + \sum_{j=0}^{i-1} C_{i-1}^j \beta^{(j)}(x_{j+1} - \hat{x}_{j+1}), \quad i = 4\end{aligned} \tag{31}$$

$$\begin{aligned}|\theta_E| &\le q_1|\beta||x_1 - \hat{x}_1| + q_2\left[\left|\dot{\beta}\right||x_1 - \hat{x}_1| + |\beta||x_2 - \hat{x}_2|\right] \\ &\quad + \cdots + q_{i-1}\sum_{j=0}^{i-2} C_{i-2}^j \left|\beta^{(j)}\right||x_{j+1} - \hat{x}_{j+1}| \\ &\quad + \sum_{j=0}^{i-1} C_{i-1}^j \left|\beta^{(j)}\right||x_{j+1} - \hat{x}_{j+1}|, \quad i = 4.\end{aligned} \tag{32}$$

According to (25) and the fact that $\beta^{(j)}, j = 0, 1, \ldots, n-1$, is bounded, it is readily shown that

$$\begin{aligned}|\theta_E| &\le q_1 |\beta| \delta b_1 + q_2 \left[\left|\dot{\beta}\right| \delta b_1 + |\beta| \delta b_2\right] + \cdots \\ &\quad + q_{i-1} \sum_{j=0}^{i-2} C_{i-2}^{j} \left|\beta^{(j)}\right| \delta b_{j+1} + \sum_{j=0}^{i-1} C_{i-1}^{j} \left|\beta^{(j)}\right| \delta b_{j+1} \\ &\le b_E, \quad i = 4.\end{aligned} \tag{33}$$

The proof is complete.

Now, we construct the following corresponding accelerated robust adaptive control strategy based on the high-gain observer:

$$u = -\left(k + \Delta k\left(\cdot\right)\right) \beta \hat{E} \tag{34}$$

where k is a positive constant as the initial value chosen by the designer, and $\Delta k(\cdot)$ is the time-varying gain updated adaptively by

$$\Delta k\left(\cdot\right) = \hat{a} \beta^2 \Phi^2 \left(\hat{Z}\right) \tag{35}$$

where $\hat{a}$ is tuned by

$$\dot{\hat{a}} = \frac{1}{2} \gamma \beta^2 \hat{E}^2 \Phi^2 \left(\hat{Z}\right) - \sigma \hat{a} \tag{36}$$

where γ and σ are the design parameters chosen by the designer.

Now, we are ready to present the following theorem that solves the contact force tracking problem for the pantograph–catenary systems essential for reliable power collection in high-speed trains.

Theorem 1: Consider the nonlinear system with external disturbances described by (2). Under Assumptions 1 and 2, if the control scheme defined by (34)–(36) is applied, not only the error e_m is ensured to be ultimately uniformly bounded (UUB), but also the tracking speed is predesignable and can be improved by choosing the rate function k_s.

C. Stability Analysis

Choose the Lyapunov function candidate as $\mathcal{V} = \frac{1}{2}E^2 + \frac{1}{2\gamma \underline{\lambda}} \tilde{a}^2$, with the parameter estimation error of the form $\tilde{a} = a - \underline{\lambda}\hat{a}$ instead of the regular form $\tilde{a} = a - \hat{a}$ and $\underline{\lambda} = \underline{\lambda}_1 \underline{\lambda}_G$; here, $\underline{\lambda}_1$ and $\underline{\lambda}_G$ are previously defined (unknown) constants.

Further differentiating $\mathcal{V}$ yields

$$\dot{\mathcal{V}} = E\beta G u + E\beta\vartheta - \frac{1}{\gamma}\tilde{a}\dot{\hat{a}} \tag{37}$$

$$\dot{\mathcal{V}} \le E\beta G u + |\beta| |\vartheta| |E| - \frac{1}{\gamma}\tilde{a}\dot{\hat{a}} \tag{38}$$

$$\dot{\mathcal{V}} \le E\beta G u + |\beta| |E| a\Phi\left(\hat{Z}\right) - \frac{1}{\gamma}\tilde{a}\dot{\hat{a}}. \tag{39}$$

Using Young's inequality, we can obtain

$$|\beta| |E| a\Phi\left(\hat{Z}\right) \le a\left(\frac{1}{4}\beta^2 E^2 \Phi^2(Z) + 1\right). \tag{40}$$

Taking into (40) and the control law, (39) becomes

$$\dot{V} \le \tfrac{1}{4} a \beta^2 E^2 \Phi^2 \left(\hat{Z}\right) + a - \left(k + \Delta k\left(\cdot\right)\right)\left(\beta E\right) G\left(\cdot\right)\left(\beta \hat{E}\right) - \tfrac{1}{\gamma}\tilde{a}\dot{\hat{a}}. \tag{41}$$

According to previous definition of $\alpha_1(t)$, we can obtain

$$-\left(\beta E\right) G\left(\cdot\right)\left(\beta \hat{E}\right) = -G\left(\cdot\right)\alpha_1(t) E^2 + G\left(\cdot\right)\alpha_1(t) E\theta_E. \tag{42}$$

Using Young's inequality, we have

$$E\theta_E \le \frac{3}{4}E^2 + \frac{1}{3}{\theta_E}^2 \le \frac{3}{4}E^2 + \frac{1}{2}{\theta_E}^2. \tag{43}$$

Inserting the bounds of $\alpha_1(t)$, $G(\cdot)$ and (44) into (42), we have

$$\begin{aligned}-(\beta E) G\left(\beta \hat{E}\right) &\le -\frac{\underline{\lambda}_1 \underline{\lambda}_G}{4} E^2 + \frac{\bar{\lambda}_1 \bar{\lambda}_G}{2} {\theta_E}^2 \\ &\le -\frac{\underline{\lambda}}{4} E^2 + \frac{\bar{\lambda}}{2} {\theta_E}^2.\end{aligned} \tag{44}$$

Then, (39) can be rewritten as

$$\begin{aligned}\dot{\mathcal{V}} \le{}& \frac{1}{4} a \beta^2 E^2 \Phi^2 \left(\hat{Z}\right) + a - \frac{\underline{\lambda}}{4}\left(k + \hat{a}\beta^2\Phi^2\left(\hat{Z}\right)\right) E^2 \\ &+ \frac{\bar{\lambda}}{2}\left(k + \hat{a}\beta^2\Phi^2\left(\hat{Z}\right)\right){\theta_E}^2 - \frac{1}{\gamma}\tilde{a}\dot{\hat{a}}.\end{aligned} \tag{45}$$

Inserting (36) and perform simple sorting, we have

$$\begin{aligned}\dot{\mathcal{V}} \le{}& \frac{1}{4}\tilde{a}\beta^2 E^2 \Phi^2\left(\hat{Z}\right) + \frac{\underline{\lambda}}{4}\hat{a}\beta^2\Phi^2\left(\hat{Z}\right) E^2 + a - \frac{\underline{\lambda}}{4} k E^2 \\ &- \frac{\underline{\lambda}}{4}\hat{a}\beta^2\Phi^2\left(\hat{Z}\right) E^2 + \frac{\bar{\lambda}}{2} k {\theta_E}^2 + \frac{\bar{\lambda}}{2}\hat{a}\beta^2\Phi^2\left(\hat{Z}\right){\theta_E}^2 \\ &- \frac{1}{2}\tilde{a}\beta^2\hat{E}^2\Phi^2\left(\hat{Z}\right) + \frac{\sigma}{\gamma}\tilde{a}\hat{a}.\end{aligned} \tag{46}$$

By using inequality $\hat{E}^2 \ge \frac{1}{2}E^2 - \theta_E^2$ and the equation $\tilde{a} = a - \underline{\lambda}\hat{a}$ to reorganize (47) again, the following inequality can be obtained:

$$\begin{aligned}\dot{\mathcal{V}} \le{}& \frac{1}{4}\tilde{a}\beta^2 E^2 \Phi^2\left(\hat{Z}\right) + a - \frac{\underline{\lambda}}{4} k E^2 + \frac{\bar{\lambda}}{2}\hat{a}\beta^2\Phi^2\left(\hat{Z}\right){\theta_E}^2 \\ &+ \frac{\bar{\lambda}}{2} k {\theta_E}^2 - \frac{1}{4}\tilde{a}\beta^2 E^2\Phi^2\left(\hat{Z}\right) + \frac{1}{2}\tilde{a}\beta^2{\theta_E}^2\Phi^2\left(\hat{Z}\right) + \frac{\sigma}{\gamma}\tilde{a}\hat{a}.\end{aligned} \tag{47}$$

The following transformation is performed on $\tilde{a}\hat{a}$, and we can get inequality (49)

$$\begin{aligned}\tilde{a}\hat{a} &= \frac{1}{\underline{\lambda}}\tilde{a}\left(a - \tilde{a}\right) = \frac{1}{\underline{\lambda}}\left(a\tilde{a} - \tilde{a}^2\right) \\ &\le \frac{1}{\underline{\lambda}}\left(\frac{1}{2}a^2 + \frac{1}{2}\tilde{a}^2 - \tilde{a}^2\right) \le \frac{1}{2\underline{\lambda}}\left(a^2 - \tilde{a}^2\right).\end{aligned} \tag{48}$$

Next, (48) can be rewritten as

$$\begin{aligned}\dot{\mathcal{V}} \le{}& -\frac{\underline{\lambda}}{4} k E^2 + a + \frac{\sigma}{2\gamma\underline{\lambda}}\left(a^2 - \tilde{a}^2\right) + \frac{\bar{\lambda}}{4} k {\theta_E}^2 \\ &+ \frac{\bar{\lambda}}{2}\hat{a}\beta^2\Phi^2\left(\hat{Z}\right){\theta_E}^2 + \frac{1}{2}\tilde{a}\beta^2{\theta_E}^2\Phi^2\left(\hat{Z}\right).\end{aligned} \tag{49}$$

Since $\tilde{a} = a - \underline{\lambda}\hat{a}$, we can get $\hat{a} = (a - \tilde{a})/\underline{\lambda}$; then, we can get

$$\dot{\mathcal{V}} \leq -\frac{\underline{\lambda}}{4}kE^2 + a + \frac{\sigma}{2\gamma\underline{\lambda}}\left(a^2 - \tilde{a}^2\right) + \frac{\bar{\lambda}}{2}k{\theta_E}^2 + \frac{1}{2}a\frac{\bar{\lambda}}{\underline{\lambda}}\beta^2\Phi^2\left(\hat{Z}\right){\theta_E}^2 - \frac{1}{2}\tilde{a}\left(\frac{\bar{\lambda}}{\underline{\lambda}} - 1\right)\beta^2\Phi^2\left(\hat{Z}\right){\theta_E}^2. \tag{50}$$

Using Young's inequality, we have

$$\begin{aligned} &-\tilde{a}\left(\tfrac{\bar{\lambda}}{\underline{\lambda}} - 1\right)\beta^2\Phi^2\left(\hat{Z}\right){\theta_E}^2 \\ &\leq \tfrac{\sigma}{2\underline{\lambda}\gamma}\tilde{a}^2 + \tfrac{\bar{\lambda}\gamma}{2\sigma}\left(\left(\tfrac{\bar{\lambda}}{\underline{\lambda}} - 1\right)\beta^2\Phi^2\left(\hat{Z}\right){\theta_E}^2\right)^2. \end{aligned} \tag{51}$$

Equation (56) can be rewritten as

$$\dot{\mathcal{V}} \leq -\frac{\underline{\lambda}}{4}kE^2 + a + \frac{\sigma}{2\gamma\underline{\lambda}}\left(a^2 - \tilde{a}^2\right) + \frac{1}{2}a\frac{\bar{\lambda}}{\underline{\lambda}}\beta^2\Phi^2\left(\hat{Z}\right){\theta_E}^2 + \frac{\bar{\lambda}}{2}k{\theta_E}^2 + \frac{\sigma}{4\underline{\lambda}\gamma}\tilde{a}^2 + \frac{\bar{\lambda}\gamma}{4\sigma}\left(\left(\frac{\bar{\lambda}}{\underline{\lambda}} - 1\right)\beta^2\Phi^2\left(\hat{Z}\right){\theta_E}^2\right)^2. \tag{52}$$

As β has an upper bound $\bar{\beta}$, and the radial basis function used herein is bounded, there is an unknown constant $b_Z > 0$ that holds $\Phi(\hat{Z}) = \|S(\hat{Z})\| + 2 \leq b_Z$.

Finally, we can obtain

$$\begin{aligned} \dot{\mathcal{V}} &\leq -\frac{\underline{\lambda}}{2}kE^2 - \frac{\sigma}{4\gamma\underline{\lambda}}\tilde{a}^2 + \frac{\sigma}{2\gamma\underline{\lambda}}a^2 + \frac{\bar{\lambda}}{2}kb_\theta{}^2 \\ &\quad + \frac{1}{2}a\frac{\bar{\lambda}}{\underline{\lambda}}\bar{\beta}^2{b_z}^2{b_\theta}^2 + \frac{\bar{\lambda}\gamma}{4\sigma}\left(\left(\frac{\bar{\lambda}}{\underline{\lambda}} - 1\right)\bar{\beta}^2{b_z}^2{b_\theta}^2\right)^2 + a \\ &\leq -\Lambda\mathcal{V} + \Theta \end{aligned} \tag{53}$$

with $\Lambda = \min\{\frac{\underline{\lambda}}{2}k, \frac{\sigma}{2}\}$ and

$$\Theta = \frac{\sigma}{2\gamma\underline{\lambda}}a^2 + \frac{\bar{\lambda}}{2}kb_\theta{}^2 + \frac{1}{2}a\frac{\bar{\lambda}}{\underline{\lambda}}\bar{\beta}^2{b_z}^2{b_\theta}^2 + \frac{\bar{\lambda}\gamma}{4\sigma}\left(\left(\bar{\lambda}/\underline{\lambda} - 1\right)\bar{\beta}^2{b_z}^2{b_\theta}^2\right)^2 + a \tag{54}$$

being constant.

Therefore, we have shown $\mathcal{V} \in \ell_\infty$; thus, $\tilde{a} \in \ell_\infty$ (also $\hat{a} \in \ell_\infty$) and $E \in \ell_\infty$, $\hat{E} \in \ell_\infty$; then, $\xi_i \in \ell_\infty, i = 1, 2, 3, 4$, $e_m \in \ell_\infty$, and $u \in \ell_\infty$.

Next, we prove that the tracking error is forced to be UUB at an accelerated rate, which can be predesigned during the tracking process.

Since $\xi_i \in \ell_\infty, i = 1, 2, 3, 4$, and $e_m = \beta^{-1}\xi_1$, then we have

$$e_m = (1 - b_f)\,{k_s}^{-1}\xi_1 + b_f\xi_1 \tag{55}$$

$$\lim_{t\to\infty} e_m = \lim_{t\to\infty}(1 - b_f)\,{k_s}^{-1}\xi_1 + b_f\xi_1 = b_f\xi_1 \in \ell_\infty \tag{56}$$

with $\lim_{t\to\infty}{k_s}^{-1} = 0$. It seen from (56) that the rate of the tracking error to be UUB can be influenced by ${k_s}^{-1}$, which can be prespecified by the designer. The proof is complete. The overall control scheme is shown in Fig. 4 , which illustrates how an output feedback neuroadaptive control is constructed to achieve stable contact force tracking for pantograph–catenary systems.

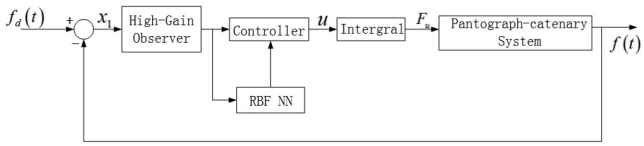

Fig. 4. Scheme of the overall system.

D. Implementation Issues

The main benefit of the proposed approach to contact force tracking control is that it offers a solution that does not rely on the precise system model and employs output feedback only, minimizing the number of sensors and thus reducing the implementation cost. In contrast, some practical issues are also worth noting in programming and especially in implementing any control strategy for active pantographs, such as measurement accuracy, actuator configuration, and high-voltage electromagnetic interference. The measurement noise, common to any control method, can be treated as additional uncertainty/disturbance attached to the system and, thus, can be accommodated with the proposed control method accordingly; the existence of measurement noise (error) of course would reduce tracking precision to some extent. The actuator configuration (location) literally affects the control gain of the system, adding additional uncertainty to the control coefficient. Interestingly, as our control method allows the control gain to be unknown and time varying, this is, therefore, not an issue in our method. High-voltage electromagnetic interference is a complicated phenomenon, resulting in additional external disturbance to the system. The robust feature of the proposed control method is deemed useful in handling such impact.

V. Numerical Simulation

In this section, we conduct numerical simulations to validate the effectiveness of the proposed controller. The model used for simulation is of the following form:

$$\begin{cases} m_1\ddot{s}_1 = -k_1(\cdot)(s_1 - s_2) - c_1(\cdot)(\dot{s}_1 - \dot{s}_2) \\ \qquad\quad -K(\cdot)\,s_1 + \sin(s_1 - s_2) + d_1(t) \\ m_2\ddot{s}_2 = k_1(\cdot)(s_1 - s_2) + c_1(\cdot)(\dot{s}_1 - \dot{s}_2) - c_2(\cdot)\,\dot{s}_2 \\ \qquad\quad +\sin(s_1 - s_2) + F_u + d_2(t) + F_L \\ f(t) = K(\cdot)\,s_1 + \frac{1}{1+s_1^2} \end{cases} \tag{57}$$

where $k_1(\cdot) = k_1 + k_{11}\sin(0.01t)$, $c_1(\cdot) = c_1 + c_{11}\sin(0.01t)$, $c_2(\cdot) = c_2 + c_{01}\sin(0.01t)$, $d_1(t) = 1 + 0.15\sin(2t)$, and $d_2(t) = 1 + 0.11\sin(2t)$. The parameters of the system are given in Table I ($k_{11} = 0.5$, $c_{01} = 1$, and $c_{11} = 1$).

The high-gain observer parameter are chosen as $\mu_1 = 2, \mu_2 = 10$, and $\mu_3 = 8$. The value of δ is generally small; in this article, we set it as 0.001. We choose the desired force as a constant $f_d = 100$ N. The control method as developed in Theorem 1 is utilized, where the control parameters are chosen as follows: $k = 20, \sigma = 0.8, \gamma = 0.001$, and $b_{if} = 0.05$, and the rate function k_s is chosen as $k_s = e^t$. The input of the NN is considered as $\hat{Z} =$

TABLE I
PANTOGRAPH–CATENARY CHARACTERISTICS

Symbol	Quantity	Value
m_1	Pan-head mass	$8kg$
c_1	Damping of the Pan-head suspension	$120Nsm^{-1}$
m_2	Frame mass	$12kg$
c_2	Damping of the frame to the base	$30Nsm^{-1}$
k_1	Pan-head suspension Stiffness	$10Nsm^{-1}$
L	Magnetization	$65m$
$K_{\max}$	Maximum value of Catenary Stiffness	$3636Nsm^{-1}$
$K_{\min}$	Minimum value of Catenary Stiffness	$3520Nsm^{-1}$
F_L	Static lift	$100N$

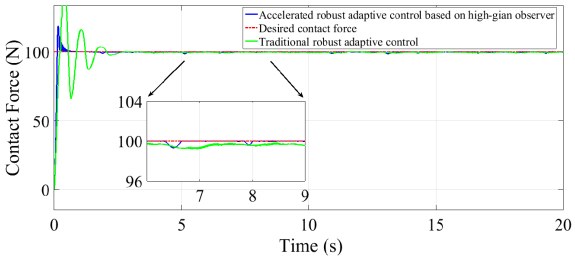

Fig. 5. Contact force tracking of proposed control method ($V =$ 200 km/h).

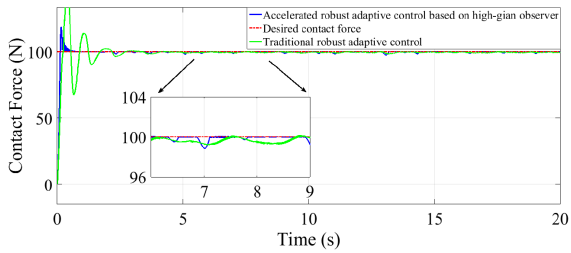

Fig. 6. Contact force tracking of proposed control method ($V =$ 350 km/h).

$[\hat{x}_1, \hat{x}_2, \hat{x}_3, \hat{x}_4]$, and the basic function is $\Phi(\hat{Z}) = \|S(\hat{Z})\| + 2$, $L_p = 50$.

The contact force tracking process under the proposed controller in comparison to the traditional control algorithm under different speeds is presented in Fig. 5 (with $V = 200$ km/h) and Fig. 6 (with $V = 350$ km/h), respectively. The traditional controller bears the same form as the proposed controller with $k_s = 1$ and, therefore, $\beta = 1$. All the other parameters are the same.

The contact force tracking error at the speed of 350 km/h is shown in Fig. 7. It is seen that although only output is utilized with the help of observer and the inevitable measurement noise (3% random noise) is added to y in the simulation, satisfactory

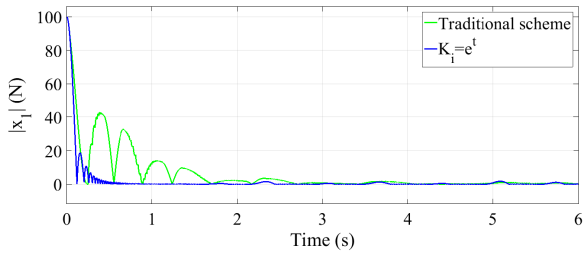

Fig. 7. Tracking error of contact force comparison between the traditional control ($k_s = 1$) and the proposed control ($k_s = e^t$) with the same design parameters.

performance is obtained with the proposed accelerate robust adaptive control method. Overall, the proposed control performs better than traditional control.

VI. CONCLUSION

This article studied the tracking control problem of the contact force between the pantograph and the catenary of high-speed trains in the presence of uncertain dynamics and external disturbances. The proposed control scheme was based on output information only and was able to regulate the force tracking error into an acceptable small region at an accelerated decaying rate, offering an inexpensive solution capable of dealing with the situation that state variables inside the system are not directly available. The developed scheme was validated via simulation. An interesting topic for future investigation is the real-time implementation and verification of the proposed method.

REFERENCES

[1] E. Karakose and M. T. Gencoglu, "An investigation of pantograph parameter effects for pantograph-catenary system," in *Proc. IEEE Int. Symp. Innov. Intell. Syst. Appl.*, Jun. 2014, pp. 338–343.
[2] J. Ambrósio, J. Pombo, and M. Pereira, "Optimization of high-speed railway pantographs for improving pantograph-catenary contact," *Theor. Appl. Mech. Lett.*, vol. 3, Jan. 2013, Art. no. 013006.
[3] Y. D. Song and X. C. Yuan, "Low-cost adaptive fault-tolerant approach for semiactive suspension control of high-speed trains,"*IEEE Trans. Ind. Electron.*, vol. 63, no. 11, pp. 7084–7093, Nov. 2016.
[4] J. Pombo, J. Ambrósio, and M. Pereira, "Influence of the aerodynamic forces on the pantograph-catenary system for high-speed trains,"*Veh. Syst. Dyn.*, vol. 47, no. 11, pp. 1327–1347, 2009.
[5] S. Midya, D. Bormann, A. Larsson, T. Schutte, and R. Thottappillil, "Understanding pantograph arcing in electrified railways—Influence of various parameter," in *Proc.IEEE Int. Symp. Electromagn. Compat.*, 2008, pp. 1–6.
[6] T. J. Park, J. W. Kim, and C. S. Han, "Dynamic sensitivity analysis for the pantograph of a high-speed rail vehicle," *J. Sound Vib.*, vol. 266, pp. 235–260, 2003.
[7] N. Mokrani, A. Rachid, and M. A. Rami, "A tracking control for pantograph-catenary system," in *Proc. 54th IEEE Conf. Decis. Control*, Dec. 2015, pp. 185–190.
[8] G. Yang, Z. M. Dai, F. Li, and Z. Z. Luo, "Active control of fuzzy for high-speed pantograph," *Appl. Mech. Mater.*, vol. 251, pp. 158–163, 2013.
[9] S. Rusu-Anghel, C. Miklos, J. Averseng, and G. O. Tirian, "Control system for catenary–pantograph dynamic interaction force," in *Proc. IEEE Int. Conf. Comput. Cybern. Tech. Informat.*, 2010, pp. 181–186.
[10] Y. Yoshitaka and I. Mitsuru, "Advanced active control of contact force between pantograph and catenary for high-speed trains," *Quart. Rep. RTRI*, vol. 53, no. 1, pp. 28–33, Feb. 2012.
[11] Y. Song, H. Q. yang, and Z. Liu, "Active control of contact force for high-speed railway pantograph-catenary based on multi-body pantograph model," *Mech. Mach. Theory*, vol. 115, pp. 35–39, Sep. 2017.

[12] C. M. Pappalardo, M. D. Patel, B. Tinsley, and A. A. Shabana, "Contact force control in multibody pantograph/catenary systems," *Proc. Inst. Mech. Eng. K, J. Multi-Body Dyn.*, vol. 230, pp. 307–328, 2016.
[13] A. Pisanoand E. Usai,"Contact force regulation in wire-actuated pantographs via variable structure control," in *Proc.46th IEEE Conf. Decis. Control*, 2007, vol. 251, pp. 1986–1992.
[14] B. Allotta, L. Pugi, and F. Bartolini, "Design and experimental results of an active suspension system for a high-speed pantograph," *IEEE/ASME Trans. Mechatron.*, vol. 13, no. 5, pp. 548–557, Oct. 2008.
[15] A. Matvejevs and A. Matvejevs, "Pantograph-catenary system modeling using MATLAB-Simulink algorithms," *Sci. J. Riga Tech. Univ. Comput. Sci.*, vol. 42, no. 1, pp. 38–44, 2010.
[16] S. S. Ge, C. C. Hang, T. H. Lee, and T. Zhang, *Stable Adaptive Neural Network Control*. Boston, MA, USA: Kluwer, 2001.
[17] A. Alberto, J. Benet, E. Ariasa, D. Cebriana, T. Rojo, and F. Cuartero, "A high performance tool for the simulation of the dynamic pantograph-catenary interaction,"*Math. Comput. Simul.*, vol. 79, no. 3, pp. 652–667, 2008.
[18] K. Zhao, Y. D. Song, and J. Y. Qian, "Zero-error tracking control with pre-assignable convergence mode for nonlinear systems under nonvanishing uncertainties and unknown control direction," *Syst. Control Lett.*, vol. 115, pp. 34–40, May 2018.
[19] J. Du, X. Hu, H. Liu, and C. L. P. Chen, "Adaptive robust output feedback control for a marine dynamic positioning system based on a high-gain observer," *IEEE Trans. Neural Netw. Learn. Syst.*, vol. 26, no. 11, pp. 2775–2786, Nov. 2015.
[20] S. Behtash, "Robust output tracking for non-linear systems," *Int. J. Control*, vol. 51, no. 6, pp. 1381–1407, 1990.
[21] Z. R. Zhang, Y. D. Song, and K. Zhao, "Neuroadaptive cooperative control without velocity measurement for multiple humanoid robots under full-state constraints," *IEEE Trans. Ind. Electron.*, vol. 66, no. 4, pp. 2956–2964, Apr. 2019.
[22] Y. D. Song, L. Y. Liang, and M. Tan, "Neuroadaptive power tracking control of wind farms under uncertain power demands," *IEEE Trans. Ind. Electron.*, vol. 64, no. 9, pp. 7071–7078, Sep. 2017.
[23] Y. D. Song, X. Huang, and Z. Jia, "Dealing with the issues crucially related to the functionality and reliability of NN-based control for nonlinear uncertain systems," *IEEE Trans. Neural Netw. Learn. Syst.*, vol. 28, no. 11, pp. 2641–2625, Nov. 2017.

Yongduan Song (Fellow, IEEE) received the Ph.D. degree in electrical and computer engineering from Tennessee Technological University, Cookeville, TN, USA, in 1992.

From 1993 to 2008, he was a tenured Full Professor with North Carolina A&T State University, Greensboro, NC, USA. From 2005 to 2008, he was a Langley Distinguished Professor with the National Institute of Aerospace, Hampton, VA, USA. He is currently the Dean of Chongqing University, Chongqing, China, where he is also the Founding Director of the Institute of Smart Systems and Renewable Energy. He has served as an Associate Editor/Guest Editor for several prestigious scientific journals. His current research interests include intelligent systems, guidance navigation and control, bioinspired adaptive and cooperative systems, and rail traffic control.

Luyuan Li received the B.S. degree in automation from Shandong University, Jinan, China, in 2017. She is currently working toward the M.S. degree in automation with the Institute of Advanced Control System, School of Electronic and Information Engineering, Beijing Jiaotong University, Beijing, China.

Her current research interests include accelerated adaptive control and pantograph–catenary systems.